

Genome-Wide Association Studies of Leaf Angle in Maize

Bo Peng (✉ snbopeng@163.com)

Tianjin Academy of Agricultural Sciences

Xiaolei Zhao

Tianjin Academy of Agricultural Sciences

Yi Wang

Tianjin Academy of Agricultural Sciences

Chunhui Li

Chinese Academy of Agricultural Sciences

Yongxiang Li

Chinese Academy of Agricultural Sciences

Dengfeng Zhang

Chinese Academy of Agricultural Sciences

Yunsu Shi

Chinese Academy of Agricultural Sciences

Yanchun Song

Chinese Academy of Agricultural Sciences

Lei Wang

Handan Academy of Agricultural Sciences

Yu Li

Chinese Academy of Agricultural Sciences

Tianyu Wang

Chinese Academy of Agricultural Sciences

Research Article

Keywords: Maize, Leaf angle, GWAS, Candidate gene

Posted Date: March 22nd, 2021

DOI: <https://doi.org/10.21203/rs.3.rs-329481/v1>

License: © ⓘ This work is licensed under a Creative Commons Attribution 4.0 International License. [Read Full License](#)

Abstract

Compact plant-type with small leaf angle has increased canopy light interception, which is conducive to the photosynthesis of the population and higher population yield at high density planting in maize. In this study, a panel of 285 diverse maize inbred lines genotyped with 56,000 SNPs was used to investigate the genetic basis of leaf angle across three consecutive years using a genome-wide association study (GWAS). The leaf angle showed broad phenotypic variation and high heritability across different years. Population structure analysis subdivided the panel into four subgroups that correspond to the four major empirical germplasm origins in China, i.e., Tangsipingtou, Reid, Lancaster and P. When tested with the optimal GWAS model, we found that the Q+K model was the best in reducing false positive. In total, 96 SNPs accounting for 5.54%-10.44% of phenotypic variation were significantly ($P < 0.0001$) associated with leaf angle across three years. According to the linkage disequilibrium decay distance, 96 SNPs were binned in 43 QTLs for leaf angle. Seven major QTLs with $R^2 > 8\%$ stably detected in at least two years and BLUP values were clustered in four genomic regions (bins 2.01, 2.07, 5.06, and 10.04). Seven important candidate genes, Zm00001d001961, Zm00001d006348, Zm00001d006463, Zm00001d017618, Zm00001d024919, Zm00001d025018, and Zm00001d025033 were predicted for the seven stable major QTLs, respectively. The markers identified in this study can be used for molecular breeding for leaf angle, and the candidate genes would contribute to further understanding of the genetic basis of leaf angle.

Introduction

Plant-type breeding with the aim of increasing tolerance to high density stress and increasing photosynthetic efficiency of populations is an important way to achieve high yield in maize. Leaf angle, which is a major factor in determining the ideal plant-type, directly affects the distribution of light and CO₂ in the canopy and the utilization of light energy of the population, and then affects the growth and development of the plant and ultimately the yield (Pendleton et al. 1968). At the high planting density, the hybrids with upright leaves always have higher grain yield than those with flat leaves (Lambert and Johnson 1978). It is one of the effective ways to increase yield by breeding ideal plant-type hybrids with suitable leaf angle in maize.

Leaf angle is a quantitative trait controlled by multiple genes with complex genetic basis in maize (Ku et al. 2012). The rapid development of DNA molecular markers and quantitative trait locus (QTL) mapping provided powerful tools for understanding the genetic basis of complex traits. Some major effect QTL ($R^2 > 10\%$) for leaf angle located in bins 1.02–1.03, 1.05, 1.09–1.10, 2.01, 2.02, 2.03, 2.07, 3.02–3.06, 5.01–5.05, 7.01, 7.02, 7.03, 8.03, 8.04, 8.05, 9.01, 9.06 and 10.07 were detected by linkage mapping in maize (Mickelson et al. 2002; Yu et al. 2006; Lu et al. 2007; Ku et al. 2010, 2012; Liu et al. 2012a; Wassom 2013; Zhang et al. 2014a; Liu et al. 2014; Chen et al. 2015; Li et al. 2015; Ding et al. 2015; Wang et al. 2017; Zhang and Huang 2021). Guo et al. (2018) collected 143 QTLs for leaf angle from the previous studies with 28 mapping populations and detected 17 mQTLs for leaf angle using the meta-analysis method. These major QTLs provide important references for map-based cloning of genes for leaf angle.

The ligular region has been proved to be the key part to regulate leaf angle (Kong et al. 2017). Biosynthesis, transport and signal transduction of plant hormones (Zhang et al. 2014b; Tian et al. 2019), and cell division and elongation in the ligular region played a crucial role in regulating the leaf angle in maize. Genes for leaf angle have been cloned mainly using mutants or homology-based cloning method in maize, for instance, *rld1*, *dwil1*, *lbi1*, *lg1*, *lg2*, *lg3*, and *lg4* (<https://www.maizegdb.org/>). *ZmTAC1* in bin 2.07–2.08, which explained 7.30% of phenotypic variation for leaf angle and was the ortholog gene of *OsTAC1* in rice, was cloned using comparative genomics (Ku et al. 2011). Only four QTLs for leaf angle have been isolated by map-based cloning (Zhang et al. 2014b; Tian et al. 2019; Ren et al. 2020). Map-based cloning was firstly used to successfully identified *ZmCLA4* on Chromosome 4 responsible for leaf angle by regulating polar auxin transport and the shape and number of cells in the ligular region (Zhang et al. 2014b). The *brd1* (brassinosteroid C-6 oxidase1) gene, which underlined the QTL on Chromosome 1 (*UPA1*), was map-based cloned and controlled leaf angle by altering endogenous brassinosteroid content (Tian et al. 2019). *UPA2*, which was a QTL for leaf angle on Chromosome 2, might repress the expression of a B3-domain transcription factor (*ZmRAVL1*) through a two-base sequence polymorphism. *ZmRAVL1* regulated the expression of *brd1* and then affecting the proliferation of cells in ligular region (Tian et al. 2019). The *ZmL11* gene underlining another QTL for leaf angle on Chromosome 2 was an ortholog of *OsL11* encoding a basic helix–loop–helix leucine zipper family transcription factor in rice (Ren et al. 2020).

Complementing the traditional linkage analysis, association mapping analysis can simultaneously evaluate the effects of multiple alleles. Moreover, association mapping analysis using diversity populations with rapid LD decline can detect the functional sequence that causes phenotypic variation in maize (Yan et al. 2011). For example, using the nesting association mapping population of maize with 4,892 RILs, Tian et al. (2011) detected 30 QTLs for leaf angle by the method of GWAS. Among them, seven SNPs in *lg1*, *lg2* and *lg4* contributed to more upright leaves. A total of 42 SNPs, which located in bins 1.02, 1.03, 1.06, 1.11, 2.05, 3.04, 5.03, 5.04, 8.03, 8.04 and 10.07, were detected significantly associated with leaf angle by the methods of GWAS in four environments using 289 maize inbred lines (Sun et al. 2018). Among them, QTLs for leaf angle located in bins 1.11, 5.03 and 8.03 could be detected in two or more environments (Sun et al. 2018). Although some QTLs/genes associated with leaf angle have been mapped and cloned in maize, there is still a lack of deep understanding of genetic bases of leaf angle.

In the present study, three GWAS models were used to analyze leaf angle across three years in maize. The objectives were to 1) characterize the phenotypic variation of leaf angle from the 285 inbred lines across three consecutive years; 2) identify SNP markers associated with leaf angle across three years, and 3) identify candidate genes for leaf angle.

Materials And Methods

Plant materials

The present study involved an diverse panel of 285 inbred lines suitable for planting in Tianjin, which were selected from three sets of inbred lines, i.e. the first from the core collection established previously by Li et al. (2004), including 242 diverse accessions which were historically used in maize breeding, the second

from research institutions or companies including 648 elite inbred lines, most of which are used in current maize breeding, and the last from 400 lines from USA, CIMMYT and Africa (Wu et al. 2015). The final maize panel included 269 lines from the three main maize production regions of China, i.e. the North China, the Huanghuaihai Valley, and the Southwest China, 24 lines from the United States, two from Africa, one from Australia and one from Mexico. The pedigrees or sources of the lines are listed in Table S1.

Phenotypic evaluation

All the 285 accessions were planted in Tianjin Academy of Agricultural Sciences Innovation Base, Wuqing, Tianjin (39°N, 117°E) in 2017, 2018, and 2019. Each line was grown in single rows 3.0 m in length with 0.6 m between rows at a planting density of 67,500 plants ha⁻¹, using a randomized complete block design with two replications per year. Five representative plants from the middle of each plot were chosen to measure the leaf angle as follows at the 10th day after anthesis. Leaf angle was measured as the angle between the vertical and the midrib of the first three leaves above ear position, and the means were used as the phenotypic data to analysis.

Phenotypic data analysis

The descriptive statistical analysis and Pearson correlation analysis for leaf angle across three years were performed using SPSS 22.0 software. Analysis of variance (ANOVA) of leaf angle across three years was performed using the *lmer* function of the lme4 package of R based on the following model: $y_{ijk} = \mu + g_i + e_j + r_k + ge_{ij} + \varepsilon_{ijk}$, where y_{ij} is the observation from the ij th plot, μ is the grand mean over all years, g_i is the genotypic effect of the i th genotype, e_j is the year effect of the j th year, r_k is the replication effect of the k th replication, ge_{ij} is the genotype \times year interaction effect, and ε_{ij} is the residual error, with genotype, year, genotype by year, and replications as random effects. The broad-sense heritability (H^2) of LA were calculated using the following formula: $H^2 (\%) = \sigma_g^2 / (\sigma_g^2 + \sigma_{ge}^2/n + \sigma_e^2/nr) \times 100\%$, where σ_g^2 is the genotypic variance, σ_{ge}^2 is the interaction variance of genotype with year, σ_e^2 is the error variance, n is the number of years, and r is the number of replications (Knapp et al. 1985). To minimize environmental effects, best linear unbiased prediction (BLUP) values for LA of each line across all years were calculated with the same ANOVA model. The BLUP values were also used as the phenotypic data of the final GWAS. The phenotypic distribution of LA across three years were performed using R software.

Genotyping and SNP filtering

The 285 lines were genotyped by MaizeSNP50 BeadChip, which included 56,110 SNPs (http://support.illumina.com/array/array_kits/maizesnp50_dna_analysis_kit.html). Totally 39,827 SNPs passed quality control *via* the software PLINK 1.90 (Purcell et al. 2007) according to the following SNP screening criteria: (1) the minor allele frequency (MAF) exceeded 0.05, and (2) the missing rate is less than 0.2. The source sequences of 39,827 SNPs were identified through BlastN search against the reference genome sequence of B73 (B73_RefGen_v4.). SNPs with ambiguous physical position or multiple blast-hits were excluded from the genotyped dataset. After that, 39,074 high-quality SNPs were used in further analysis.

Population structure analysis

The model-based clustering algorithm of ADMIXTURE v1.3 was used (Alexander et al. 2009) to investigate subpopulation structure of the 285 maize accessions. A subset of 6,527 genome-wide SNP markers filtered by PLINK v.1.90 software using the parameters `-indep-pairwise 50 10 0.5`, `MAF \geq 0.05` and `missing data < 5%` were used. A preliminary analysis was performed in multiple runs by inputting successive values of K from 1 to 10. A 5-fold CV procedure was performed for each K -value. The most likely K -value was determined using ADMIXTURE's CV values. The stacked bar-charts were plot using `barplot` command in the R software. Inbred lines with membership probabilities of more than 0.5 were assigned to corresponding clusters (Liu et al. 2012).

To obtain an in-depth picture of the genetic relationships among 285 inbred lines, the genetic distance between pair-lines was calculated by using 3,9074 SNPs. Modified Euclidean was defined as follows: $D = 1 - \text{identity by state (IBS) similarity}$ (Legesse et al. 2007). IBS means the probability that alleles derived at random from two individuals at identical loci are the same. For any two lines, the probability of IBS was averaged over all non-missing loci. The cladogram was constructed based on the distance matrix described above based on the neighbor-joining (NJ) algorithm. Clusters were observed from the result of the phylogenetic tree. All calculations were carried out in TASSEL software 5.2.69 (Bradbury ET AL. 2007). Principal component analysis with 39,074 SNPs of the 285 individuals was carried out using the TASSEL software 5.2.69.

Linkage disequilibrium analysis

Linkage disequilibrium (LD) was assessed using PopLDdecay 3.40 software (<https://github.com/BGI-shenzhen/PopLDdecay>) and a perl script, respectively (Zhang et al. 2018). The average r^2 value was calculated using 39,074 SNPs with `MAF > 0.05` and `missing data < 20%`.

Association study and candidate gene identification

Principal component analysis (PCA) was implemented in TASSEL 5.2.69, and the top five principal components were used to estimate the population structure matrix to control population structure. Kinship matrices were calculated using the Dominance-Normalized-IBS method in TASSEL 5.2.69 to estimate genetic relatedness among individuals. To balance false negative and false positive SNPs in GWAS, three models were performed in TASSEL 5.0: (1) Q model: GLM (General Linear Model) + PCA, (2) K model: MLM (Mixed Linear Model) + Kinship; (3) Q + K model: MLM + PCA + kinship. The quantile-quantile plots (QQ plot) obtained from each analysis were plotted using the R software, and the optimal statistical model was identified for the GWAS analysis. Because several SNPs should be in LD, the GEC software tool (Li et al. 2012) was used to calculate the effective number of independent SNPs (N_e). The recommended threshold ($1/N_e$) calculated by the software was used as the basis for the significant correlation between LA and SNPs.

Based on the average LD decay across the whole genome, significant SNPs within the LD decay distance were binned into one QTL, and the most significant SNP were selected as the lead SNP. All the potential candidate genes within LD decay distance upstream and downstream of the lead SNP of all QTLs were identified from Gramene database (<http://ensembl.gramene.org/>) based on the maize B73 RefGen_V4 genome. The biological functions of the candidate genes were predicted from Gramene database, maize GDB database (<http://www.maizegdb.org>) and Gene Ontology database. In addition, some candidate genes were also annotated by the homologous genes in rice (RAP database) or *Arabidopsis thaliana* (Tair database). Combined with the above gene annotation and related literatures, the most possible candidate gene for leaf angle was identified in each QTL interval.

Results

Phenotypic variation and heritability of leaf angle

The basic statistical analysis for leaf angle of the 285 inbred lines showed that extensive and continuous variation were conserved for leaf angle in different years, and the variation range of leaf angle in 2017 and 2018 was larger than that in 2019 and BLUP for the three years (Fig. 1, Table 1). It indicated that the leaf angle was a typical quantitative trait and was controlled by polygenes. The variances of genotype (σ^2_g), year (σ^2_y) and genotype \times year (σ^2_{gy}) were significant at $P < 0.01$, and the broad-sense heritability of leaf angle was 93.94% (Table 2). Significant correlation ($P < 0.01$) for leaf angle among three years and BLUP values ($r^2 = 0.79-0.97$) was also observed. It indicated that leaf angle was mainly controlled by genetic factors.

Table 1
Basic statistical analysis and correlation coefficients of leaf orientation value across three years

Year	Mean	Range	Std. Dev	Skewness	Kurtosis	Pearson's correlation coefficient		
						2017	2018	2019
2017	20.92	2.90-67.65	10.27	1.02	1.62			
2018	21.80	4.05-66.95	12.15	1.15	1.32	0.91**		
2019	24.67	7.15-61.30	9.28	0.76	0.63	0.83**	0.79**	
BLUP	22.43	6.93-62.70	9.34	1.03	1.34	0.97**	0.96**	0.91**
* and ** indicate significance at $P < 0.05$ and $P < 0.01$, respectively								

Table 2
Analysis of variance (ANOVA) for leaf angle across three years

Variation source	Variance	H^2 (%)
Genotype (σ^2_g)	92.98**	
Year (σ^2_y)	3.79**	
Genotype \times Year (σ^2_{gy})	7.15**	93.94
Replication	85.7	
Residual	21.71	
* and ** indicate significance at $P < 0.05$ and $P < 0.01$, respectively		

Model-based population structure population structure and relative kinship

A total of 39,074 high-quality SNPs were mapped in the reference genome B73_RenGen_v4, and the number of SNPs on individual chromosome ranged from 2754 on Chromosome 10 to 6259 on Chromosome 1 (Fig. S1). When counting the number of SNPs per 1 Mb across the whole genome, the distribution density of SNPs at both ends of each chromosome was relatively high, while the distribution density of SNPs near the centromere was relatively low. The highest density region contained 63 SNPs/Mb, and the lowest contained 1 SNPs/Mb. The average SNP density was 20 SNPs/Mb across the whole genome.

The populations of 285 accessions based on the model-based algorithm were analyzed using the even distribution of 6527 SNPs. As the ADMIXTURE software overestimated the number of subgroups for inbred lines because Chinese maize inbred lines derived from Chinese landraces and U.S. hybrids often have complex genetic background, and it was difficult to choose the "correct" K from the cross-validation error of data (Fig. 2A). Thus, the results were compared with the known pedigree of the inbred lines for each run of different Ks. The results showed that when K = 4, the model-based subgroups were largely consistent with known pedigrees of the inbred lines. The four groups corresponded to the four major germplasm origins in China, i.e., Tangsipingtou (TSPT), Reid, Lancaster and P (Fig. 2B; Table S1).

The TSPT group was the largest group with 91 inbred lines, which were mainly derived from Huangzaosi, one of the founder parents in maize breeding of China. In addition, some lines derived from the landrace of Ludahonggu and the inbred line of "Zi330" were also designed into this group. The Reid group included 56 inbred lines, which were mainly selected from Pioneer hybrids "3382" and "U8". The Lancaster group included 41 inbred lines, which were mainly derived from "Mo17" and "Va35". The P group included 32 inbred lines, which were mainly derived from the Pioneer hybrid of "P78599". Additionally, 65 inbred lines that had 0.5 membership in each of the five subgroups and had a mixture of two or more subgroups were assigned to a mixed subgroup (Table S1).

Estimation of relative kinships showed that 94.16 % of paired relative kinship ranged from 0.05 to 0.30, 0.33 % of paired relative kinship equaled to 0, and 1.16 % of paired relative kinship ranged from 0 to 0.05 (Fig. 3). This analysis indicated that a weak or various relative kinship existed in this collection of germplasm.

Neighbor-joining tree and principal component analysis

A neighbor-joining tree was constructed based on the modified Euclidean distance and is shown in Fig. 4. The 285 accessions were firstly clustered into three major groups according to their origins: TSPT, the mixed group of P and Reid, and Lancaster, which contained 81, 125 and 79 accessions, respectively. The TSPT group could be further clustered into two major subgroups according to their origins: the Chang7-2 cluster with 45 lines and the Zi330 cluster with 36 lines. The P + Reid group was then clustered into the Ye8112 cluster including 61 lines, the 599 cluster including 51 lines, and the Va35 cluster including 13 lines. The Lancaster group could be clustered into two subpopulations, i.e. the C416 cluster with 39 lines and the Fengke1 cluster with 40 lines (Fig. 4). These results showed moderately common with some difference compared to that evaluated by using model-based method.

The PCA results showed obvious population differences among the groups of TSPT, Reid, Lancaster and P and a good agreement with both model-based population structure and clustering analyses (Fig. 5). The 95% confidence intervals of Lancaster and TSPT partly overlapped. Which may be resulted by the larger introgression existing between Lancaster and TSPT accessions, and lower power of PCA in population structure analysis by using only two PCs. The representative lines Chang7-2, Ye8112, and 599 for TSPT, Reid, and P groups exhibited obvious differentiation.

Linkage disequilibrium analysis

The LD decay indicated that the mean of r^2 in the panel dropped rapidly at approximately 10 Kb, and The mean of r^2 at 27.5 Kb was 0.2 (Fig. S2). The average LD decay distance was 383 kb in the panel. Combined with the average LD decay distance and the physical location of peak SNP, the candidate genes at each QTL can be further inferred.

Genome-wide association analysis

The effective marker number of 39,074 high quality SNPs was analyzed by using the GEC software. The results showed that the effective marker number N_e was 24166, and the suggested P value was $4.14E-5$, that is, $-\log P$ was 4.38. Therefore, this value was used as the threshold for significant marker-trait association in the whole genome association analysis of leaf angle.

The leaf angles in the three years and their BLUP values were analyzed by GWAS using three models (Q, K and Q + K). QQ diagram showed that Q model and K model had high type I errors (false positive), while Q + K model was the best in reducing false positive (Fig. 6). Therefore, a mixed linear model based on Q + K model was used for leaf angle genome-wide association analysis.

Genome-wide association analysis was carried out for the leaf angles across the three consecutive years and their BLUP values of 285 diversity inbred lines combined with 39074 SNPs markers covering the genome. A total of 96 SNPs significantly associated with leaf angle were detected based on the Q + K model ($P < 4.14E-5$), which were distributed on all chromosomes except Chr. 8 (Fig. 7, Table S2). Based on the average LD decay distance across the whole genome, 96 SNPs significantly associated with leaf angle were distributed in 43 QTLs, ranging from one QTL (Chr. 3) to nine QTLs (Chr. 2).

In the present study, the QTLs contained SNP with $R^2 > 8\%$ in at least one year were considered as major QTLs, and the major QTLs detected in at least 2 years and also for BLUP values were called "stable major QTLs". Thus, seven stable major QTLs located in four chromosome segments of bin 2.01, bin 2.07, bin 5.06 and bin 10.04 were detected (Fig. 7, Table 3).

Table 3
Significant SNPS and candidate genes associated with leaf orientation value identified by GWAS across three years

Bin	Year	SNP	Physical position ^b	P value	R ² (%)	Lead SNP physical Position ^b	QTL region ^b		Candidate gene	Gene annotation	
							-LD	+LD			
11	2.01	BLUP	SYN9223	3825340	2.57E-06	8.99	3825340	3442340	4208340	Zm00001d001961	SAUR-auxin-respon protein
11	2.01	LA17	SYN9223	3825340	2.70E-05	7.18					
11	2.01	LA18	SYN9223	3825340	2.70E-06	9.29					
11	2.01	LA19	SYN9223	3825340	1.89E-05	7.67					
17	2.07	BLUP	PZE-102152182	205338006	1.07E-07	9.24	205338006	204955006	205721006	Zm00001d006348	Growt regula factor
17	2.07	LA17	PZE-102152182	205338006	3.09E-07	8.38					
17	2.07	LA18	PZE-102152182	205338006	7.33E-07	8.13					
17	2.07	LA19	PZE-102152182	205338006	3.16E-07	8.84					
18	2.07	BLUP	PUT-163a-18167719-1296	209342747	2.12E-05	6.81	209322345	208939345	209705345	Zm00001d006463	C2C2-transc factor
18	2.07	LA17	PUT-163a-18167719-1296	209342747	3.05E-05	6.50					
18	2.07	LA18	PUT-163a-18167719-1296	209342747	2.51E-05	6.75					
18	2.07	LA19	PZE-102155296	209322345	7.51E-06	8.10					
29	5.06	BLUP	PZE-105142621	201997615	1.28E-06	9.01	201997615	201614615	202380615	Zm00001d017618	ABI3-transc factor
29	5.06	LA17	PZE-105142621	201997615	1.08E-06	9.03					
29	5.06	LA18	PZE-105142621	201997615	2.66E-06	8.69					
41	10.04	BLUP	ZM009620-0299	94989318	2.22E-06	7.54	94989318	94606318	95372318	Zm00001d024919	Adeny kinase
41	10.04	LA18	ZM009620-0299	94989318	4.72E-07	8.69					
41	10.04	LA19	ZM009620-0299	94989318	9.31E-06	6.79					
42	10.04	BLUP	PZE-110052645	99718797	1.69E-05	6.99	99821364	99438364	100204364	Zm00001d025018	alpha expan
42	10.04	BLUP	PZE-110052727	99821364	2.62E-06	8.37					
42	10.04	LA17	PZE-110052727	99821364	2.50E-05	6.79					
42	10.04	LA18	PZE-110052645	99718797	1.83E-06	8.54					
42	10.04	LA18	PZE-110052727	99821364	1.24E-07	10.44					
43	10.04	BLUP	PZE-110053215	100548773	3.74E-07	9.99	100593657	100210657	100976657	Zm00001d025033	TCP-transc factor
43	10.04	BLUP	SYN18673	100593657	1.81E-07	8.95					

^a Based on the average LD decay across the whole genome, significant SNPs within the LD decay distance were binned into one QTL;^bphysical position based on B73_RefGen_v4.

43	10.04	BLUP	SYN18670	100593728	3.61E-07	8.78
43	10.04	BLUP	PZE-110053293	100650632	3.78E-06	6.74
43	10.04	LA17	PZE-110053215	100548773	3.32E-06	8.34
43	10.04	LA17	SYN18673	100593657	1.87E-06	7.35
43	10.04	LA17	SYN18670	100593728	1.83E-06	7.61
43	10.04	LA17	PZE-110053293	100650632	5.76E-06	6.40
43	10.04	LA18	PZE-110053215	100548773	2.58E-06	8.78
43	10.04	LA18	SYN18673	100593657	6.10E-07	8.25
43	10.04	LA18	SYN18670	100593728	1.67E-06	7.89
43	10.04	LA18	PZE-110053293	100650632	1.57E-06	7.31
43	10.04	LA18	PZE-110053348	100768927	3.25E-05	6.53
43	10.04	LA19	PZE-110053215	100548773	5.58E-07	10.02
43	10.04	LA19	SYN18673	100593657	3.38E-07	8.77
43	10.04	LA19	SYN18670	100593728	1.07E-06	8.26

^a Based on the average LD decay across the whole genome, significant SNPs within the LD decay distance were binned into one QTL;^b physical position based B73_RefGen_v4.

The first stable major QTL was QTL11 located in bin 2.01. This locus could be detected in all three years and joint analysis (BLUP), explaining 7.18% – 9.29% of the phenotypic variation for leaf angle.

Two stable major QTLs, QTL17 and QTL18, were both detected in bin 2.07. The two QTLs could be detected in all three years and for their BLUP values, explaining 8.13%-9.24% and 6.50%-8.10% of the phenotypic variation for leaf angle, respectively.

The fourth stable major QTL (QTL29) was located in bin 5.06 and could be detected in 2017, 2018 and for BLUP values, explaining 8.69%-9.01% of the phenotypic variation for leaf angle.

Three stable major QTLs (QTL41, QTL42 and QTL43), including 24 SNPs significantly associated with leaf angle, were detected in bin 10.04. QTL41 was detected in 2018, 2019 and for BLUP values, explaining 6.79% -8.69% of the phenotypic variation for leaf angle. Both QTL42 and QTL43 could be detected in three years and their BLUPs, explaining 6.79% – 10.44% and 6.40% – 10.02% of the phenotypic variation for leaf angle, respectively.

Prediction of candidate genes for leaf angle

Candidate genes within the range of LD decay distance between the upstream and downstream of a given lead SNP were identified for each QTL. The most promising candidate gene was predicted for each of 43 QTLs for leaf angle (Table 3, Table S2). The candidate genes are mainly related to the imbalanced division or expansion of the adaxial and abaxial cells in the ligular region, the biosynthesis and signal transduction of plant hormones such as brassinosteroid, auxin, cytokinin and ethylene, the strength of mechanical tissue in the ligular region, and development-related transcription factors.

Discussion

Population structure of the 285 diverse inbred lines in China

The main heterotic groups according to the pedigree information in China varied with different stages, that is Golden Queen, Huobai, TSPT, Ludahonggu and Lancaster in 1970s (Wu 1983); TSPT, Ludahonggu, Lancaster, and Reid in 1980s (Zeng 1990); Lancaster (Mo17 subgroup and Zi330 subgroup), Reid, TSPT, Ludahonggu and other germplasm in 1990s (Wang et al. 1998; Teng et al. 2004); Reid, P, Ludahonggu, TSPT, Lancaster in early 2000s (Teng et al. 2004; Sun et al. 2014). Recently, SS, NSS and X groups were generated with the hybrids of Monsanto and Pioneer companies introduced to China (Sun et al. 2014; Zhao et al. 2018a). The main heterotic groups of China were also determined by molecular evaluation (Xie et al. 2007, 2008; Wang et al. 2008; Wu et al. 2014a). A mini core set of 95 lines which represented the Chinese maize inbred lines were assigned to four groups, i.e., TSPT, Reid, Lancaster, and P group (Wang et al. 2008). Wu et al. (2014a) also subdivided 367 inbred lines historically and recently widely used in maize breeding of China into Reid, Lancaster, P, TSPT, and Tem-

tropic I group. In the present study, 285 inbred lines were assigned to four major groups by the model-based method and PCA, i.e., TSPT, Reid, Lancaster, and P group, which were consistent with known pedigrees of the inbred lines and previous studies (Wang et al. 2008; Wu et al. 2014a).

The TSPT group played a dominant role in Chinese maize breeding and occupied an important position in Chinese maize heterotic patterns. For example, Zhengdan958 derived from the pattern of Reid × TSPT was the most important Chinese maize hybrid with the largest annual planting area in consecutive 16 years since 2004. Ludan981 derived from P × TSPT with annual planting area about 0.67 million hectares from 2004 to 2007. Some elite lines of Chinese maize breeding historically and currently, such as Chang7-2, Dan340 and Aijin525 were developed from Chinese landraces (Li and Wang 2010), most of which and their descendants were clustered into the TSPT group in the present study. These results were consistent with Xie et al. (2007, 2008), who integrated the Ludahonggu and TSPT group into the D group. The reciprocal genetic improvement of TSPT and other local germplasm e.g. Ludahonggu and Golden queen were also founded based on the pedigree of some excellent lines, i.e., 5237 derived from Huangzaosi × Dan340 (TSPT × Ludahonggu), Jing2416 derived from 5237 × Jing24, Xun92_8 derive from Chang7-2 × 5237, and Shuang741 derived from [(3Tuan-11 × Huafeng100) × Huangzaosi] × Aijin525. In additionally, Zi330 and its descendants were also always used to improve lines from TSPT by Chinese breeders. For example, Ji853, a famous parent in TSPT, was derived from Huangzaosi × Zi330. Furthermore, several reports classified Zi330 and Ludahonggu into one group (Teng et al. 2004; Wang et al. 2008). Therefore, lines from Ludahonggu, Zi330 and local landraces were important donors to improve the TSPT germplasm.

Complex genetic basis of Lancaster was confirmed by the present study. Some lines of Lancaster according to pedigree were assigned to TSPT and P + Reid by neighbor-joining tree analysis, such as lines from the Zi330 subgroup and the Va35 subgroup. The PCA results also showed that the Lancaster germplasm generally close to other germplasm. One reason was that the Lancaster Surecrop germplasm was less than 50% in the lines of Lancaster in China (Zheng et al. 2002).

The Reid group still occupied an important position in Chinese maize heterotic patterns. The Reid germplasm, such as M14, W24, W59E and B73, were firstly introduced to China in the 1950s. Later, using a batch of hybrids introduced from the United States, such as XL80, 3147, U8 and 3382, Chinese breeders developed several excellent inbred lines, such as Ye107, U8112, Ye478, Tie7922, Shen5003 (Li and Wang 2010). Recently, the female parent of Denghai605, the fourth Chinese maize hybrids with planting area more than 0.85 million hectares in 2019, was also derived from Reid.

The P inbreds, such as 178, P138, 87001, Qi319, Dan598, Dan599, Ye107 and 18–599, have been developed from the Pioneer hybrid of “78599” or similar hybrids since the late 1980s (Xie et al. 2007, 2008; Li and Wang 2010). Due to the existence of tropical and subtropical germplasm in the P group, the resistance to biotic and abiotic stress is often strong. Therefore, the introgression of the P germplasm to Reid, SS or NSS germplasm attracted more attention of breeders. Recent years, the success of several hybrids with extensive planting in China, e.g. Denghai605, Yufeng303 and Zhongkeyu505, were partly attributed to the P germplasm.

Comparative analysis of the genetic basis for leaf angle

The heritability of leaf angle varied, depending on genetic populations and environments in which populations are evaluated. It was found that the heritability of leaf angle was 90.5% in different years (Wassom 2013), 54.56%–87.00% at different locations (Michelson et al. 2002; Chen et al. 2015; Ding et al. 2015), 68.00%–81.15% in different years combined with locations (Ku et al. 2010; Li et al. 2015). In addition, the heritability of leaf angle was 84.00% (Wang et al. 2017) under different planting densities (52500 plants/ha, 67500 plants/ha and 82500 plants/ha). Except that the heritability of leaf angle in Xiema, Beibei and Hechuan in Chongqing was 54.56–58.75% (Chen et al. 2015), more than 68.00% was observed for the heritability of leaf angle in different environments in other reports. In this study involving 285 diverse inbred lines of maize, it was found that the heritability of leaf angle was also very high (93.94%), indicating that Leaf angle was mainly controlled by genetic factors and less influenced by environments.

Zhao et al. (2018b) integrated the results of 27 QTL mapping studies for leaf angle, leaf orientation, leaf length, leaf width, leaf area and leaf length/width, and 16 meta-QTLs (mQTLs) were found to be distributed on 8 chromosomes except Chr. 9 and Chr. 10, suggesting the complexity of the genetic basis of leaf angle in maize. In this study, a total of 96 SNPs significantly associated with leaf angle ($P < 4.14E-5$) were distributed in 27 bins on the nine chromosomes except Chr. 8. We further identified 43 QTLs for leaf angles, of which 7 stable major QTLs (explaining more than 8% of the phenotypic variation for leaf angle and could be stably detected in at least 2 years and also for BLUP values) were distributed in bin 2.01, bin 2.07, bin 5.06 and bin 10.04.

QTL11 located in bin 2.01 were also identified by Lu et al. (2007), Ding et al. (2015), Li et al. (2015), and Wang et al. (2017) using different linkage mapping populations, explaining 2.86%, 4.06%, 4.30%, 8.85% of phenotypic variation, respectively. Ku et al. (2012) and Zhao et al. (2018b) integrated the previous QTLs for leaf angle, and detected an mQTL in bin 2.01 by meta-analysis. This locus in bin 2.01 stably expressed in different environments and different genetic backgrounds might be an important target for further study on leaf angle.

Two stable major QTLs (QTL17 and QTL18) were detected in bin 2.07, and a total of 8 SNPs significantly associated with leaf angle within these two QTLs could be stably inherited in different years. Liu et al. (2012a) detected a major QTL explaining 10.8% of phenotypic variation for leaf angle in bin 2.02–2.07. Zhang and Huang (2021) also found a major QTL in bin 2.07, which accounted for 14.2% of phenotypic variation for leaf angle. Due to the limited number of parents, the interaction of QTL × genetic background, population size and marker density in linkages analysis, and population structure and rare alleles in association analysis, few studies identified QTLs for leaf angle in this bin.

QTL29 located in bin 5.06 was a hot spot locus for leaf angle founded by previous studies (Michelson et al. 2002; Lu et al. 2007; Zhang et al. 2014a; Zhao et al. 2018b), and could explain 4.17%–9.40% of phenotypic variation. In addition, Ku et al. (2012) integrated the previous QTL mapping results of leaf angle, and found an mQTL in bin 5.06 by meta-analysis. The mQTL affected both leaf angle and leaf orientation, and four candidate genes, *yabby9*, *SE*, *LIC* and *yabby15* were predicted. Therefore, bin 5.06 might play an important role in leaf angle.

In previous studies, QTLs for leaf angle detected were mainly located in bin 10.07 (Yu et al. 2006; Zhang et al. 2014a; Sun et al. 2018; Wang et al. 2017), while bin 10.01–10.02 (Zhao et al. 2018b), bin 10.06 (Li et al. 2015) and bin 10.08–10.09 (Yu et al. 2006) were also reported. However, the QTL in bin 10.04 was the most important locus found in the present study, which carried three stable major QTLs (QTL41, QTL42 and QTL43), and contained 24 SNPs significantly associated with leaf angle. Therefore, the present study found for the first time that bin 10.04 plays an important role in the regulation of leaf angle in maize, and there may be at least three major genes that control leaf angle within this region. It was necessary to further map-based clone the genes underline by constructing large-scale secondary segregation populations.

Analysis of candidate genes for leaf angle

In recent years, a few genes regulating leaf angle or tiller angle were cloned in rice, maize, etc. It has been clear that leaf ligular region is the key tissue to regulate leaf angle (Zhu et al. 2015; Kong et al 2017; Hu et al. 2019). Factors such as the imbalanced division and expansion of adaxial and abaxial cells, the strength of mechanical tissue and the gravity response in the ligular region will affect the leaf angle (Zhu et al. 2015; Hu et al. 2019). The molecular regulation mechanism of leaf angle mainly including (1) the regulatory pathway of plant hormone synthesis and signal transduction: brassinosteroid, auxin and gibberellin have been deeply studied on the regulation of leaf angle, while other hormones such as jasmonic acid, strigolactones and ethylene have also been found to be involved in the regulation of ligular region development. (2) other regulatory pathways: the gravity response of the ligular region (such as *LPA1*, which affects the division of adaxial cells in ligular region, and *LAZY1*, which regulates the polar auxin transport) or the strength of mechanical tissue in ligular region (such as *ILA1*, which controls the formation of vascular bundles and the content of cellulose and xylan in the cell wall; *OsCesA7* and *OsCD1* involved in cellulose synthesis; *DL*, the YABBY gene family, which controls the formation of leaf blade-midribs; *OsIG1* involved in the division and differentiation of vesicular cell and the formation of ligular region). (Zhu et al. 2015; Luo et al. 2016; Hu et al. 2019)

The progress of identifying the regulatory genes for leaf angle in maize is relatively slow. Through the research on mutants, a few genes in regulating leaf angle was cloned, such as *LG1*, encoding squamosa promoter binds to protein (SBP); *LG2*, encoding a basic leucine zipper protein (bZIP); *Ig3* and *Ig4*, encoding homeo domain protein. The mutants of *Ig1* and *Ig2* (Moreno et al. 1997; Walsh et al. 1998) and the dominant mutants of *Ig3-O* and *Ig4-O* showed that the abnormal development of ligular region resulted in a small leaf angle (Bauer et al. 2004). Through homologous cloning, *ZmTAC1*, a homologous gene of *TAC1* that regulated leaf angle in rice, had been proved to be able to positively regulate the leaf angle (Ku et al. 2011). In recent years, *ZmCLA4* underlined *qLA4-1* in bin 4.03 (Zhang et al. 2014b), *brd1* underlined *UPA1* in bin 1.08 and two-base sequence polymorphism underlined *UPA2* in bin 2.03 (Tian et al. 2019), and *ZmML1* underlined *qLA2* in bin 2.02 (Ren et al. 2020) for leaf angle have successively map-based cloned. Seven stable major QTLs for leaf angle were identified in the present study, which will be useful for the improvement of leaf angle by molecular breeding and provide a basis for the cloning of the genes.

The candidate gene of QTL11 might be Zm00001d001961, which encoded SAUR-like auxin-responsive protein. The majority of SAUR genes can induce growth in leaves, stems and floral organs via cell elongation (Sun et al. 2016; Stortenbeker and Bemer 2019). In addition, the overexpression of SAUR could also influence the auxin levels, polar auxin transport and/or expression of auxin pathway genes (Stortenbeker and Bemer 2019). Auxin can also played role on the leaf angle via the regulation of the growth of the abaxial and adaxial cells of ligular region, auxin signal transduction (Song et al. 2009; Li et al. 2010). So Zm00001d001961 might regulate leaf angle by the division and expansion of adaxial and abaxial cells.

Zm00001d006348, the predicted candidate gene for QTL17, encoded a growth-regulating factor (GRF) with two conserved domains, i.e. WRC and QLQ (Choi et al. 2004). Through the interaction between QLQ domain in the N-terminal of GRFs and the SNH domain in GIF (GRF-interaction factor) protein, a functional complex which regulated the expression of genes downstream was formed (Kim and Kende 2004). In *Arabidopsis thaliana*, GRFs could promote or inhibit the growth of organs by regulating the cell size (Kim et al 2003) or the cell division (Kim and Lee 2006; Vercruyssen et al. 2015). Over-expression of *BrGRF8* from Chinese cabbage (Wang et al. 2014) and *BnGRF2* from rapeseed (Liu et al 2012b) in transgenic *Arabidopsis* plants increased the sizes of the leaves and other organs by regulation of cell proliferation. It was also found that genes for GRFs could regulate several traits, such as leaf size, plant height and flowering traits in maize (Wu et al 2014b; Zhang et al. 2008). Their transcriptional expression were affected by gibberellin (GA) (Wang et al. 2014) and miR396 (Jones-Rhoades et al. 2006). Because the protein encoded by the candidate gene of Zm00001d006348 was the homologous sequence of that encoded by *AT2G45480* (GROWTH-REGULATING FACTOR 9) in *Arabidopsis thaliana*, the function of Zm00001d006348 can be predicted by *AT2G45480*. *AT2G45480* negatively regulated leaf growth by activating the expression of a bZIP transcription factor gene, i.e. *OBP3-RESPONSIVE GENE (ORG3)*, and restricted cell proliferation in the early stage of leaf development (Omidbakhshfard et al. 2018). Therefore, Zm00001d006348 might negatively regulate the proliferation of cells in the ligular region, and further affect the leaf angle.

Zm00001d006463, the candidate gene for QTL18, encoded C2C2-Dof-transcription factor with a highly conserved DNA-binding domain of Cys2/Cys2 (C2/C2) zinc finger (Yanagisawa, 2004). The DOF proteins were found involved in many biological processes, such as tissue differentiation, seed development and regulation of metabolism (Noguero et al. 2013). It is worth noting that the DOF transcription factor AtDOF5.1 could regulate leaf adaxial-abaxial polarity by controlling the expression of *Revoluta (REV)*, a Class III homeodomain-leucine zipper (HD-ZIP III) transcriptional regulatory proteins (Kim et al. 2010). Therefore, Zm00001d006463 might also regulate the leaf adaxial-abaxial polarity in maize.

Zm00001d017618, a possible candidate gene for QTL29, encoded a B3-domain transcription factor that might regulate the expression of genes in the BR synthesis pathway and the signal transduction pathway (Tian et al. 2019; Je et al. 2010). Recently, Tian et al. (2019) found that the B3-domain transcription factor gene Zm00001d002562 (*ZmRAVL 1*) on Chrom. 2 activated the expression of *brd1* downstream, increased endogenous brassinosteroid content, promoted proliferation of cells in ligular region, and enlarged leaf angle. Therefore, Zm00001d017618 was predicted to regulate the leaf angle via brassinosteroid content in the ligular region.

Zm00001d024919 encoding an adenylate kinase was the possible gene for QTL41. Two near isogenic lines with different leaf angle were analyzed by the method of comparative proteomic analysis, and adenylate kinase complicated in glycometabolism might be associated with leaf angle formation and the

physical and mechanical properties of midribs (Wang et al. 2015).

The candidate gene for QTL42 might be Zm00001d025018 encoding alpha expansin. Expansins responsible for cell-wall relaxation are required for cell elongation (Kong et al. 2017). Furthermore, increased expansin expression at early stages of organ development induced cell proliferation and consequently increased growth (Wyrzykowska et al. 2002). Both the size of the cells determined by the cell elongation and the number of cells determined by the cell division influence the size of the auricle and ultimately leaf angle (Kong et al. 2017).

Zm00001d025033 encoding a TCP transcription factor was the possible candidate gene of QTL43. TCP transcription factors with TCP conserved domain formed a bHLH structure had been found to regulate many aspects of plant development, such as branching in maize (Doebley 1995; Bai et al. 2012). *tb1* (*Teosinte Branched 1*) can inhibit the growth and development of lateral branches, and *tb1* mutant gene led to increased number of lateral branches in maize (Doebley 1995). *BAD1*, which is another TCP transcription factor gene and could promote cell proliferation in a lateral organ, i.e. the ligular region, may influence inflorescence architecture by regulating the angle of lateral branch emergence (Bai et al. 2012). Zm00001d025036 encoding indole-3-acetate beta-glucosyltransferase also located in this QTL. The glycosylation of auxin might influence the phenotype of plant via the regulation of auxin levels (Jackson et al. 2002).

Supplementary information

Declarations

Authors' contributions TW, YL and CL conceived the project and provided the genotype of diverse inbred lines; XZ and YW conducted the field experiments and collected the phenotypic data, BP implemented all data collection, analysis and wrote this manuscript; CL, YL, DZ, YS, YS, LW, YL, and TW participated in its design and coordination and helped to draft the manuscript. All authors had read and approved the final manuscript.

Funding This work was supported by the National Natural Science Foundation of China (31601308), the Tianjin Natural Science Foundation (19JCZDJC34500) and the Innovative Research and Experiment Project for Young Researchers of Tianjin Academy of Agricultural Sciences (2021018).

Ethics approval and consent to participate Not applicable.

Consent for publication Not applicable.

Availability of data and material Not applicable.

Code availability Not applicable.

Competing interests The authors declare no competing interests.

References

- Alexander DH, Novembre J, Lange K (2009) Fast model-based estimation of ancestry in unrelated individuals. *Genome Res* 19:1655–1664. <https://doi.org/10.1101/gr.094052.109>
- Bai F, Reinheimer R, Durantini D, Kellogg EA, Schmidt RJ (2012) TCP transcription factor, BRANCH ANGLE DEFECTIVE 1 (BAD1), is required for normal tassel branch angle formation in maize. *Proc Natl Acad Sci USA*: 109:12225–12230. <https://doi.org/10.1073/pnas.1202439109>
- Bauer P, Lubkowitz M, Tyers R, Nemoto K, Meeley RB, Goff SA, Freeling M (2004) Regulation and a conserved intron sequence of *liguleless3/4* *knox* class-I homeobox genes in grasses. *Planta* 219:359–368. <https://doi.org/10.1007/s00425-004-1233-6>
- Bradbury PJ, Zhang Z, Kroon DE, Casstevens TM, Ramdoss Y, Buckler ES (2007) TASSEL: software for association mapping of complex traits in diverse samples. *Bioinformatics* 23:2633–2635. <https://doi.org/10.1093/bioinformatics/btm308>
- Chen X, Xu D, Liu Z, Yu T, Mei X, Cai Y (2015) Identification of QTL for leaf angle and leaf space above ear position across different environments and generations in maize (*Zea mays* L.). *Euphytica* 204:395–405. <https://doi.org/10.1007/s10681-015-1351-1>
- Choi D, Kim JH, Kende H (2004) Whole genome analysis of the Os-GRF gene family encoding plant-specific putative transcription activators in rice (*Oryza sativa* L.). *Plant Cell Physiol* 45:897–904. <https://doi.org/10.1093/pcp/pch098>
- Ding J, Zhang L, Chen J, Li X, Li Y, Cheng H, Huang R, Zhou B, Li Z, Wang J, Wu J (2015) Genomic dissection of leaf angle in maize (*Zea mays* L.) using a four-way cross mapping population. *PLoS One* 10:e0141619. <https://doi.org/10.1371/journal.pone.0141619>
- Doebley J, Stec A, Gustus C (1995) *Teosinte branched 1* and the origin of maize: Evidence for epistasis and the evolution of dominance. *Genetics* 141:333–346
- Guo SL, Zhang J, Qi JS, Yue RQ, Han XH, Yan SF, Lu CX, Fu XL, Chen NN, Ku LX, Tie SG (2018) Analysis of meta-quantitative trait loci and candidate genes related to leaf shape in maize. *Bulletin of Botany* 53:487–501. <https://doi.org/10.11983/CBB17082>
- Hu J, Lin H, Xu N, Jiao R, Dai ZJ, Lu CL, Rao YC, Wang YX (2019) Advances in molecular mechanisms of rice leaf inclination and its application in breeding. *Chin J Rice Sci*: 391–400. <https://doi.org/10.16819/j.1001-7216.2019.9029>
- Jackson RG, Kowalczyk M, Li Y, Higgins G, Ross J, Sandberg G, Bowles DJ (2002) Over-expression of an *Arabidopsis* gene encoding a glucosyltransferase of indole-3-acetic acid: phenotypic characterisation of transgenic lines. *Plant J* 32:573–583. <https://doi.org/10.1046/j.1365-313x.2002.01445.x>
- Je BI, Piao HL, Park SJ, Park SH, Kim CM, Xuan YH, Park SH, Huang J, Choi YD, An G, Wong HL, Fujioka S, Kim MC, Shimamoto K, Han C (2010) *RAV-Like1* maintains brassinosteroid homeostasis via the coordinated activation of *BRI1* and biosynthetic genes in rice. *Plant Cell* 22:1777–1791.

<https://doi.org/10.1105/tpc.109.069575>

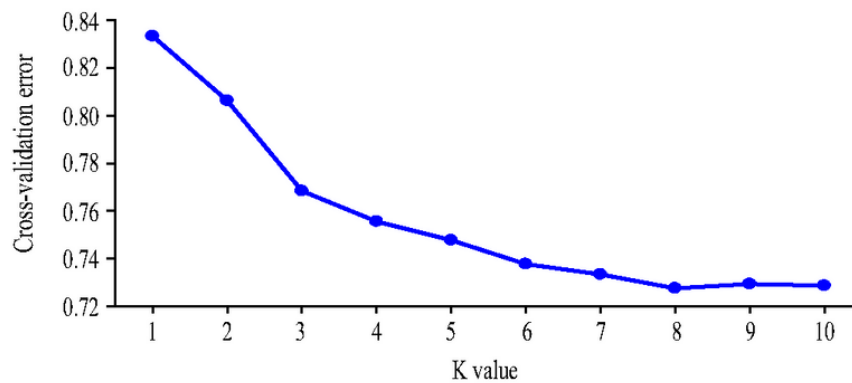
13. Jones-Rhoades MW, Bartel DP, Bartel B (2006) MicroRNAs and their regulatory roles in plants. *Annu Rev Plant Biol* 57:19–53. <https://doi.org/10.1146/annurev.arplant.57.032905.105218>
14. Kim HS, Kim SJ, Abbasi N, Bressan RA, Yun DJ, Yoo SD, Kwon SY, Choi SB (2010) The DOF transcription factor Dof5.1 influences leaf axial patterning by promoting *Revoluta* transcription in *Arabidopsis*. *Plant J* 64:524–535. <https://doi.org/10.1111/j.1365-313X.2010.04346.x>
15. Kim JH, Choi D, Kende H (2003) The AtGRF family of putative transcription factors is involved in leaf and cotyledon growth in *Arabidopsis*. *Plant J* 36:94–104. <https://doi.org/10.1046/j.1365-313x.2003.01862.x>
16. Kim JH, Kende H (2004) A transcriptional coactivator, AtGIF1, is involved in regulating leaf growth and morphology in *Arabidopsis*. *Proc Natl Acad Sci USA* 101:13374–13379. <https://doi.org/10.1073/pnas.0405450101>
17. Kim JH, Lee BH (2006) GROWTH-REGULATING FACTOR4 of *Arabidopsis thaliana* is required for development of leaves, cotyledons, and shoot apical meristem. *J Plant Biol* 49:463–468. <https://doi.org/10.1007/BF03031127>
18. Knapp SJ, Stroup WW, Ross WW (1985) Exact confidence intervals for heritability on a progeny mean basis. *Crop Sci* 25:192–194. <https://doi.org/10.2135/cropsci1985.0011183X002500010046x>
19. Kong F, Zhang T, Liu J, Heng S, Shi Q, Zhang H, Wang Z, Ge L, Li P, Lu X, Li G (2017) Regulation of leaf angle by auricle development in maize. *Mol Plant* 10:516–519. <https://doi.org/10.1016/j.molp.2017.02.001>
20. Ku LX, Zhang J, Guo SL, Liu HY, Zhao RF, Chen YH (2012) Integrated multiple population analysis of leaf architecture traits in maize (*Zea mays* L.). *J Exp Bot* 63:261–274. <https://doi.org/10.1093/jxb/err277>
21. Ku LX, Zhao WM, Zhang J, Wu LC, Wang CL, Wang PA, Zhang WQ, Chen YH (2010) Quantitative trait loci mapping of leaf angle and leaf orientation value in maize (*Zea mays* L.). *Theor Appl Genet* 121:951–959. <https://doi.org/10.1007/s00122-010-1364-z>
22. Lambert RJ, Johnson RR (1978) Leaf angle, tassel morphology, and the performance of maize hybrids. *Crop Sci* 18:499–502. <https://doi.org/10.2135/cropsci1978.0011183X001800030037x>
23. Legesse BW, Myburg AA, Pixley KV, Botha AM (2007) Genetic diversity of African maize inbred lines revealed by SSR markers. *Hereditas* 144:10–17. <https://doi.org/10.1111/j.2006.0018-0661.01921.x>
24. Li C, Li Y, Shi Y, Song Y, Zhang D, Buckler ES, Zhang Z, Wang T, Li Y (2015) Genetic control of the leaf angle and leaf orientation value as revealed by ultra-high density maps in three connected maize populations. *PLoS One* 10:e0121624. <https://doi.org/10.1371/journal.pone.0121624>
25. Li LC, Kang DM, Chen ZL, Qu LJ (2010) Hormonal regulation of leaf morphogenesis in *Arabidopsis*. *J Integr Plant Biol* 49:75–80. <https://doi.org/10.1111/j.1744-7909.2006.00410.x>
26. Li MX, Yeung JM, Cherny SS, Sham PC (2012) Evaluating the effective numbers of independent tests and significant *P*-value thresholds in commercial genotyping arrays and public imputation reference datasets. *Hum Genet* 131:747–756. <https://doi.org/10.1007/s00439-011-1118-2>
27. Li Y, Shi YS, Cao YS, Wang TY (2004) Establishment of a core collection for maize germplasm preserved in Chinese National GenBank using geographic distribution and characterization data. *Genet Resour Crop Evol* 51:845–852. <https://doi.org/10.1007/s10722-005-8313-8>
28. Li Y, Wang TY (2010) Germplasm base of maize breeding in China and formation of foundation parents. *J Maize Sci* 5:1–8. <https://doi.org/CNKI:SUN:YMKX.0.2010-05-003>
29. Liu J, Hua W, Yang HL, Zhan GM, Li RJ, Deng LB, Wang XF, Liu GH, Wang HZ (2012a) The *BnGRF2* gene (*GRF2-like* gene from *Brassica napus*) enhances seed oil production through regulating cell number and plant photosynthesis. *J Exp Bot* 63: 3727–3740. <https://doi.org/10.1093/jxb/ers066>
30. Liu PF, Jiang F, Wang HN, Wang XM (2012b) QTL mapping for leaf angle and leaf orientation in corn. *J Nucl Agric Sci* 26:231–237. <https://doi.org/CNKI:SUN:HNXB.0.2012-02-008>
31. Liu Z, Yu TT, Mei XP, Chen XN, Wang GQ, Wang JG, Liu CX, Wang X, Cai YL (2014) QTL mapping for leaf angle and leaf space above ear position in maize (*Zea mays* L.). *J Agric Biotech* 22:177–187. <https://doi.org/10.3969/j.issn.1674-7968.2014.02.006>
32. Lu M, Zhou F, Xie CX, Li MS, Xu YB, Warburton M, Zhang SH (2007) Construction of an SSR linkage map and mapping of quantitative trait loci (QTL) for leaf angle and leaf orientation with an elite maize hybrid. *Hereditas (Beijing)* 29:1131–1138. <https://doi.org/10.1360/yc-007-1131>
33. Luo XY, Zheng JS, Huang YM, Huang HC, Wang LG, Fang XJ (2016) Phytohormones signaling and crosstalk regulating leaf angle in rice. *Plant Cell Rep* 35:2423–2433. <https://doi.org/10.1007/s00299-016-2052-5>
34. Mickelson SM, Stuber CS, Senior L, Kaepler SM (2002) Quantitative trait loci controlling leaf and tassel traits in a B73×Mo17 population of maize. *Crop Sci* 42:1902–1909. <https://doi.org/10.2135/cropsci2002.1902>
35. Moreno MA, Harper LC, Krueger RW, Dellaporta SL, Freeling M (1997) *1guleless1* encodes a nuclear-localized protein required for induction of ligules and auricles during maize leaf organogenesis. *Genes Dev* 11:616–628. <https://doi.org/10.1101/gad.11.5.616>
36. Noguero M, Atif RM, Ochatt S, Thompson RD (2013) The role of the DNA-binding One Zinc Finger (DOF) transcription factor family in plants. *Plant Sci* 209:32–45. <https://doi.org/10.1016/j.plantsci.2013.03.016>
37. Omidbakhshfard MA, Fujikura U, Olas JJ, Xue GP, Balazadeh S, Mueller-Roeber B (2018) GROWTH-REGULATING FACTOR 9 negatively regulates *Arabidopsis* leaf growth by controlling *ORG3* and restricting cell proliferation in leaf primordia. *PLoS Genet* 14:e1007484. <https://doi.org/10.1371/journal.pgen.1007484>
38. Pendleton JW, Smith GE, Winter SR, Johnston TJ (1968) Field investigations of the relationships of leaf angle in corn (*Zea mays* L.) to grain yield and apparent photosynthesis. *Agron J* 60:422–424. <https://doi.org/10.2134/agronj1968.00021962006000040027x>
39. Purcell S, Neale B, Todd-Brown K, Thomas L, Ferreira M, Bender D, Maller J, Sklar P, de Bakker PIW, Daly MJ, Sham PC (2007) PLINK: a tool set for whole-genome association and population-based linkage analyses. *Am J Hum Genet* 81:559–575. <https://doi.org/10.1086/519795>

40. Ren Z, Wu L, Ku L, Wang H, Zeng H, Su H, Wei L, Dou D, Liu H, Cao Y, Zhang D, Han S, Chen Y (2020) *ZmL17* regulates leaf angle by directly affecting *liguleless1* expression in maize. *Plant Biotechnol J* 18:881–883. <https://doi.org/10.1111/pbi.13255>
41. Song Y, You J, Xiong L (2009) Characterization of *OsAA1* gene, a member of rice *Aux/IAA* family involved in auxin and brassinosteroid hormone responses and plant morphogenesis. *Plant Mol Biol* 70:297–309. <https://doi.org/10.1007/s11103-009-9474-1>
42. Stortenbeker N, Bemer M (2019) The SAUR gene family: the plant's toolbox for adaptation of growth and development. *J Exp Bot* 70:17–27. <https://doi.org/10.1093/jxb/ery332>
43. Sun J, Zhao MA, Pan SX, Pei YH, Guo XM, Song XY (2018) Correlation analysis of maize leaf angle with genome-wide association analysis. *Acta Agric Boreali-Sin* 33:60–64. <https://doi.org/10.7668/hbxb.2018.01.010>
44. Sun Q, Li WC, Zhang FJ, Yu YL, Zhang QW, Dou SQ, Meng ZD (2014) Analysis on the number of maize hybrids which approved by the nation from 2001 to 2012 and the usage of base inbred lines. *J Maize Sci* 4: 39–43. <https://doi.org/CNKI:SUN:YMKX.0.2014-06-002>
45. Teng WT, Cao JS, Chen YH, Liu XH, Jing XQ, Zhang FJ, Li JS (2004) Analysis of maize heterotic groups and patterns during past decade in China. *Sci Agric Sin* 12:1804–1811. <https://doi.org/10.3321/j.issn:0578-1752.2004.12.004>
46. Tian F, Bradbury PJ, Brown PJ, Hung H, Sun Q, Flint-Garcia S, Rocheford TR, McMullen MD, Holland JB, Buckler ES (2011) Genome-wide association study of leaf architecture in the maize nested association mapping population. *Nat Genet* 43:159–162. <https://doi.org/10.1038/ng.746>
47. Tian J, Wang C, Xia J, Wu L, Xu G, Wu W, Li D, Qin W, Han X, Chen Q, Jin W, Tian F (2019) Teosinte ligule allele narrows plant architecture and enhances high-density maize yields. *Science* 365:658–664. <https://doi.org/10.1126/science.aax5482>
48. Vercruyssen L, Tognetti VB, Gonzalez N, Dingenen JV, Milde LD, Bielach A, Rycke RD, Breusegem FV, Inzé D (2015) GROWTH REGULATING FACTOR5 stimulates *Arabidopsis* chloroplast division, photosynthesis, and leaf longevity. *Plant Physiol* 167:817–832. <https://doi.org/10.1104/pp.114.256180>
49. Walsh J, Waters CA, Freeling M (1998) The maize gene *liguleless2* encodes a basic leucine zipper protein involved in the establishment of the leaf blade-sheath boundary. *Genes Dev* 12:208–218. <https://doi.org/10.1101/gad.12.2.208>
50. Wang F, Qiu N, Ding Q, Li J, Zhang Y, Li HY, Gao J (2014) Genome-wide identification and analysis of the growth-regulating factor family in Chinese cabbage (*Brassica rapa* L. ssp. *pekinensis*). *BMC Genom* 15:807. <https://doi.org/10.1016/j.gene.2017.09.070>
51. Wang HW, Liang QJ, Li K, Hu XJ, Wu YJ, Wang H, Liu ZF, Huang CL (2017) QTL analysis of ear leaf traits in maize (*Zea mays* L.) under different planting densities. *Crop J* 5: 387–395. <https://doi.org/CNKI:SUN:CROP.0.2017-05-004>
52. Wang N, Cao D, Gong F, Ku L, Chen Y, Wang W (2015) Differences in properties and proteomes of the midribs contribute to the size of the leaf angle in two near-isogenic maize lines. *J Proteomics* 128:113–122. <https://doi.org/10.1016/j.jprot.2015.07.027>
53. Wang RH, Yu YT, Zhao JR, Shi YS, Song YC, Wang TY, Li Y (2008) Population structure and linkage disequilibrium of a mini core set of maize inbred lines in China. *Theor Appl Genet* 117:1141–1153. <https://doi.org/10.1007/s00122-008-0852-x>
54. Wang YB, Wang ZH, Lu LX, Wang YP, Zhang X, Tian ZY (1998) Studies on maize germplasm base, division of heterosis groups and utilizing models of heterosis in China. *J Maize Sci* 1:9–13. <https://doi.org/CNKI:SUN:YMKX.0.1998-01-002>
55. Wassom JJ (2013) Quantitative trait loci for leaf angle, leaf width, leaf length, and plant height in a maize (*Zea mays* L.) B73 × Mo17 population. *Maydica* 58:318–321
56. Wu JF (1983) A review on the germplasm bases of the main corn hybrids in China. *Sci Agric Sin* 2:1–8
57. Wu L, Zhang DF, Xue M, Qian JJ, He Y, Wang SC (2014b) Overexpression of the maize GRF10, an endogenous truncated growth-regulating factor protein leads to reduction in leaf size and plant height. *J Integr Plant Biol* 56:1053–1063. <https://doi.org/10.1111/jipb.12220>
58. Wu X, Li Y, Li X, Li C, Shi Y, Song Y, Zheng Z, Li Y, Wang T (2015) Analysis of genetic differentiation and genomic variation to reveal potential regions of importance during maize improvement. *BMC Plant Biol* 15:256. <https://doi.org/10.1186/s12870-015-0646-7>
59. Wu X, Li YX, Shi YS, Song YC, Wang TY, Huang YB, Li Y (2014a) Fine genetic characterization of elite maize germplasm using high-throughput SNP genotyping. *Theor Appl Genet* 127:621–631. <https://doi.org/10.1007/s00122-013-2246-y>
60. Wyrzykowska J, Pien S, Shen WH, Fleming AJ (2002) Manipulation of leaf shape by modulation of cell division. *Development* 129:957–964. <https://doi.org/10.1113/expphysiol.2006.035253>
61. Xie CX, Warburton M, Li MS, Li XH, Xiao MJ, Hao ZF, Zhao Q, Zhang SH (2008) An analysis of population structure and linkage disequilibrium using multilocus data in 187 maize inbred lines. *Mol Breed* 21:407–418. <https://doi.org/10.1007/s11032-011-9556-z>
62. Xie CX, Zhang SH, Li MS, Li XH, Hao ZF, Bai L, Zhang DG, Liang YH (2007) Inferring genome ancestry and estimating molecular relatedness among 187 Chinese inbred lines. *J Genet Genomics* 34:738–748. [https://doi.org/10.1016/S1673-8527\(07\)60083-6](https://doi.org/10.1016/S1673-8527(07)60083-6)
63. Yan J, Warburton M, Crouch J (2011) Association mapping for enhancing maize (*Zea mays* L.) genetic improvement. *Crop Sci* 51:433–449. <https://doi.org/10.2135/cropsci2010.04.0233>
64. Yanagisawa S (2004) Dof domain proteins: plant-specific transcription factors associated with diverse phenomena unique to plants. *Plant Cell Physiol* 45: 386–391. <https://doi.org/10.1093/pcp/pch055>
65. Yu Y, Zhang J, Shi Y, Song Y, Wang T, Li Y (2006) QTL analysis for plant height and leaf angle by using different populations of maize. *J Maize Sci* 14:88–92. <https://doi.org/10.1360/yc-006-1280>
66. Zeng SX (1990) The maize germplasm base of hybrids in China. *Sci Agric Sin* 4:1–9
67. Zhang DF, Li B, Jia GQ, Zhang TF, Dai JR, Li JS, Wang SC (2008) Isolation and characterization of genes encoding GRF transcription factors and GIF transcriptional coactivators in maize (*Zea mays* L.). *Plant Sci* 175:809–817. <https://doi.org/10.1016/j.plantsci.2008.08.002>

68. Zhang J, Ku LX, Han ZP, Guo SL, Liu HJ, Zhang ZZ, Cao LR, Cui XJ, Chen YH (2014a) The *ZmCLA4* gene in the *qLA4-1* QTL controls leaf angle in maize (*Zea mays* L.). *J Exp Bot* 65:5063–5076. <https://doi.org/10.1093/jxb/eru271>
69. Zhang N, Huang X (2021) Mapping quantitative trait loci and predicting candidate genes for leaf angle in maize. *PLoS One* 16:e0245129. <https://doi.org/10.1371/journal.pone.0245129>
70. Zhang ZL, Liu PF, Jiang F, Chen QC, Zhang Y, Wang XM, Wang HN (2014b) QTL mapping for leaf angle and leaf orientation in maize using a four-way cross population. *J China Agric Univ* 19: 7–16. <https://doi.org/CNKI:SUN:NYDX.0.2014-04-003>
71. Zhao JR, Li CH, Song W, Wang YD, Zhang RY, Wang JD, Wang FG, Tian HL, Wang (2018a) Genetic diversity and population structure of important Chinese maize breeding germplasm revealed by SNP-Chips. *Sci Agric Sin* 4:626–634. <https://doi.org/10.3864/j.issn.0578-1752.2018.04.003>
72. Zhao X, Fang P, Zhang J, Peng Y (2018b) QTL mapping for six ear leaf architecture traits under water-stressed and well-watered conditions in maize (*Zea mays* L.). *Plant Breed* 137:60–72. <https://doi.org/10.1111/pbr.12559>
73. Zheng DH, Li YR, Jin FX, Jiang JJ (2002) Pedigree and germplasm base of inbreds of the Lancaster heterotic group of maize in China. *Sci Agric Sin* 7:750–757. <https://doi.org/CNKI:SUN:ZGNX.0.2002-06-000>
74. Zhu LP, Zou J, Chen XB (2015) Research progress in molecule regulation mechanism of leaf inclination angle in rice (*Oryza sativa* L.). *Chemistry of Life* 35:589–595. <https://doi.org/CNKI:SUN:SMHX.0.2015-04-022>

Figures

A



B

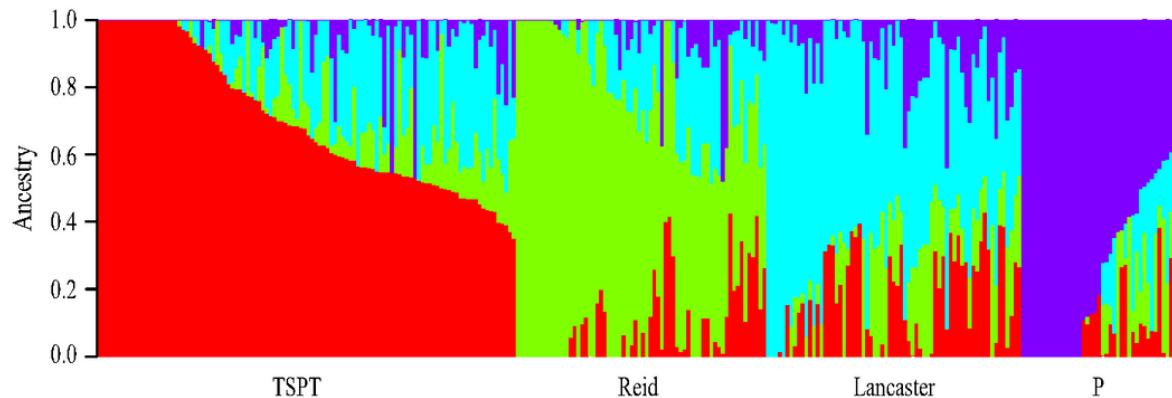


Figure 1

Distribution of phenotypic values of leaf angle in the association mapping population across three years

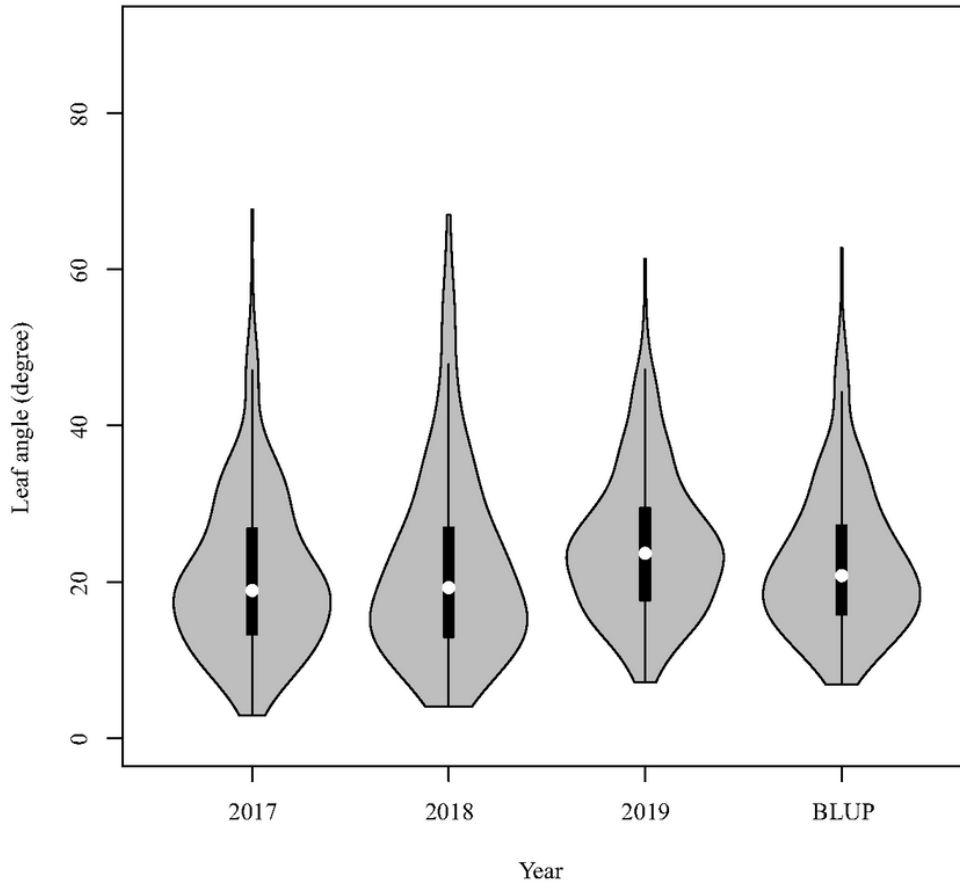


Figure 2
Population structure analysis of 285 maize accessions A: The cross-validation for K values from 1 to 10 using 6527 unlinked ($r^2 > 0.5$) SNPs distributed across the genome. B: Hierarchical organization of genetic relatedness of the 285 maize accessions, each individual bar represents an accession

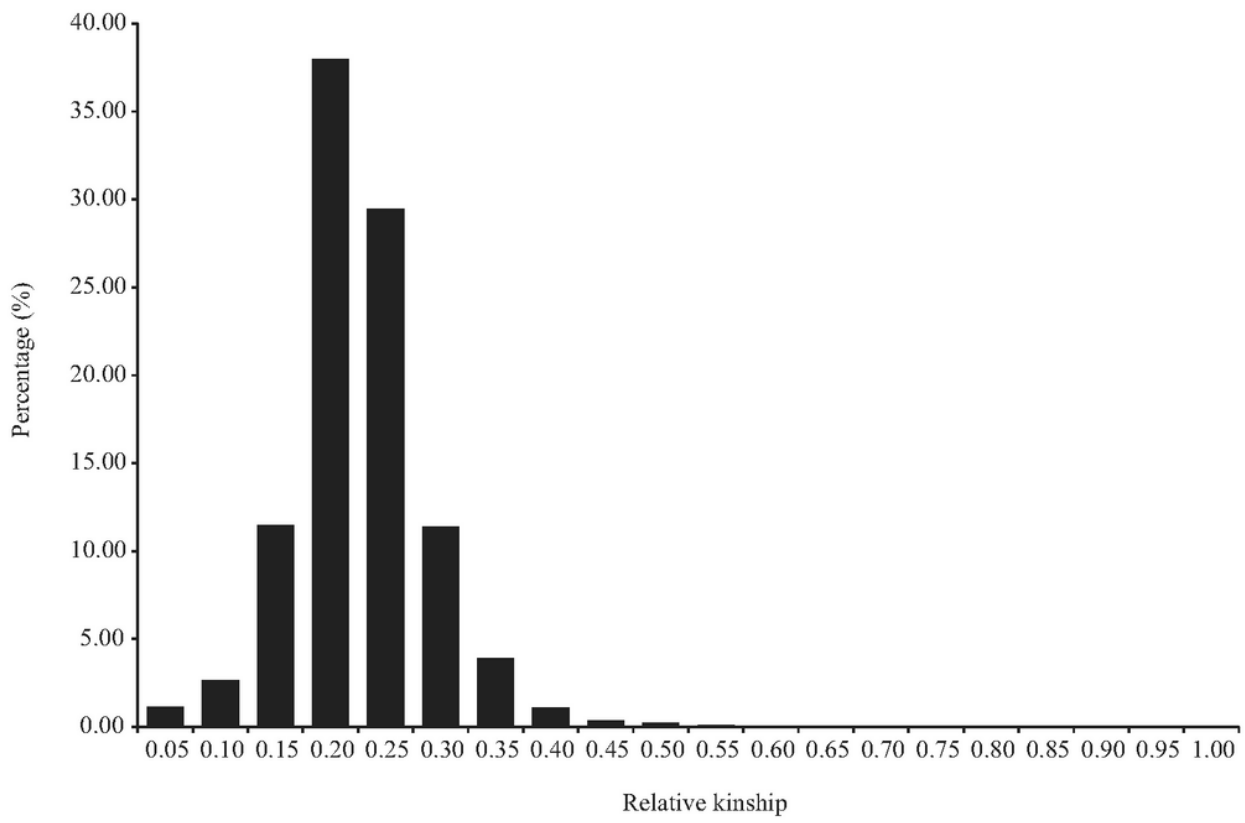


Figure 3

Distribution of paired kinship evaluated between the 285 lines

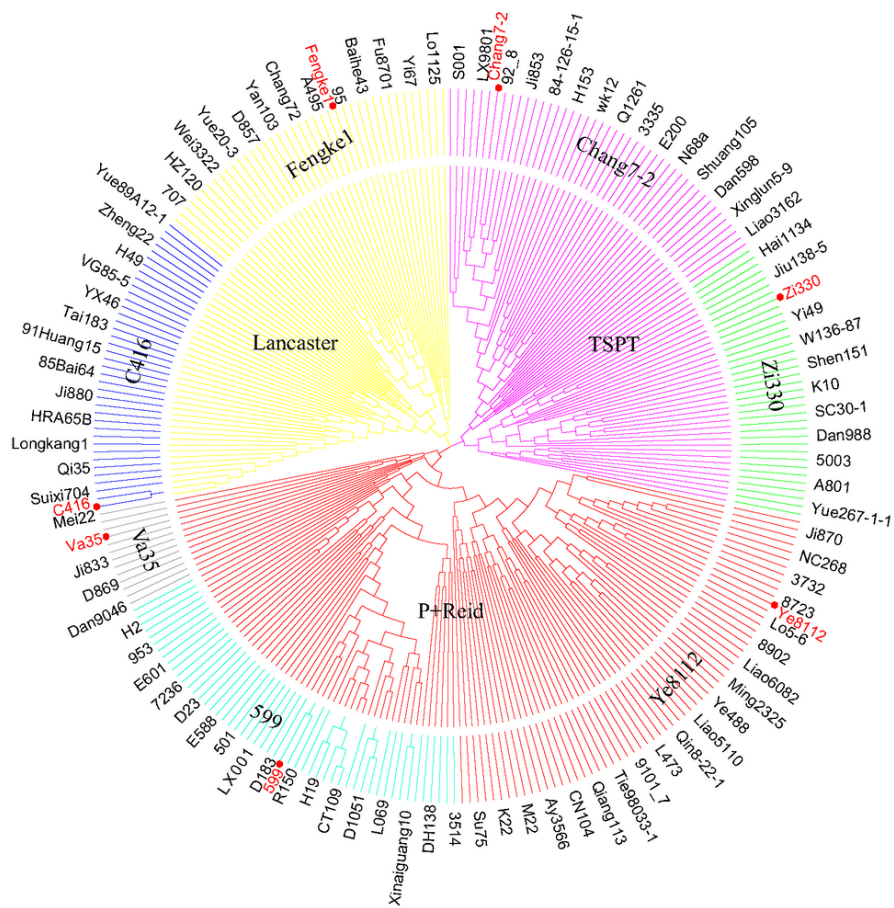


Figure 4

Neighbor-joining trees of the 285 maize accessions Chang7-2 is a representative inbred of the Tangsipingtou group (TSPT). Zi330, Va35, C416 and Fengke1 are representative inbreds of the Lancaster group. Ye8112 and 599 are representative inbreds of the Reid group and the P group, respectively.

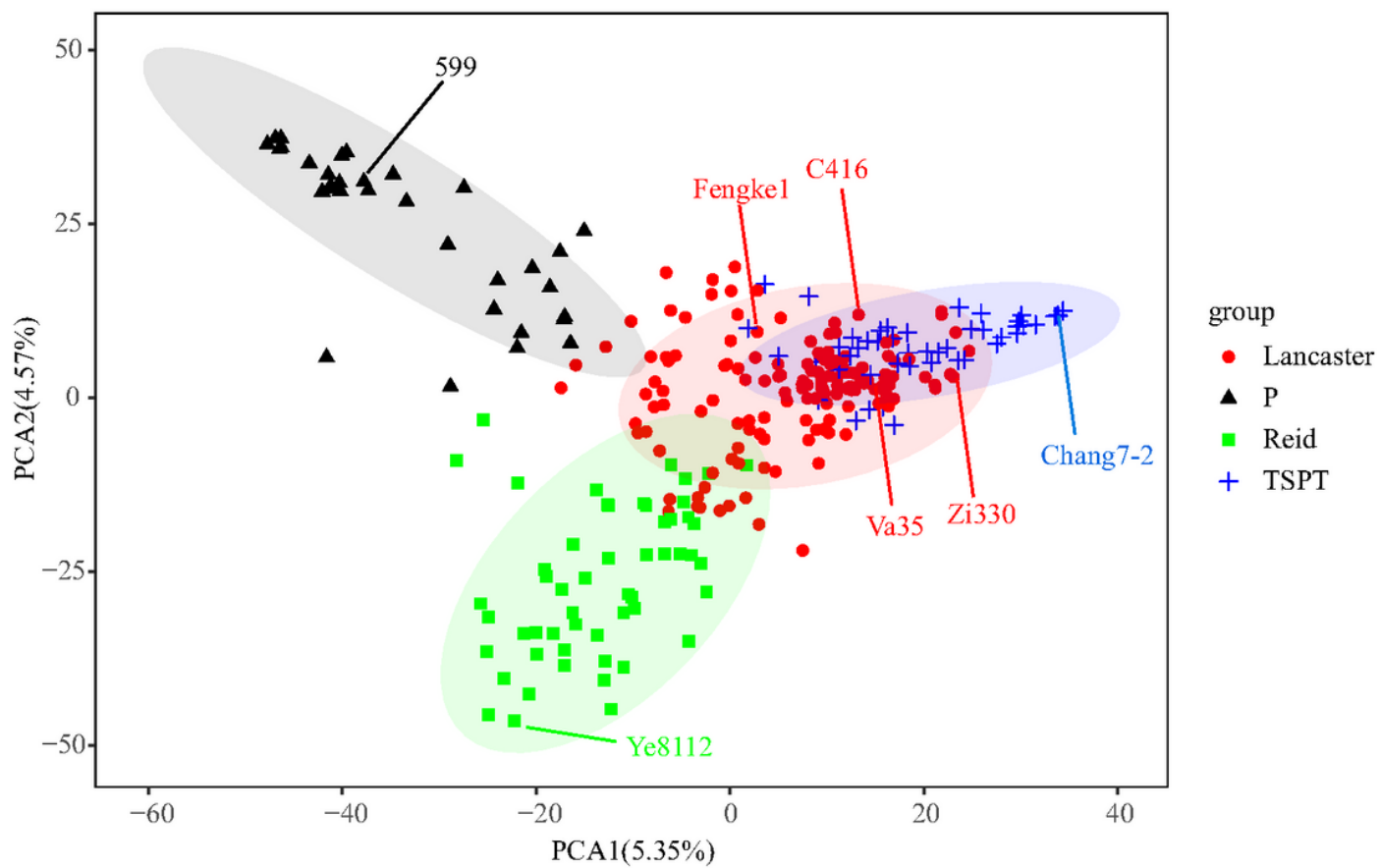


Figure 5
 Results of principal component analysis (PCs)

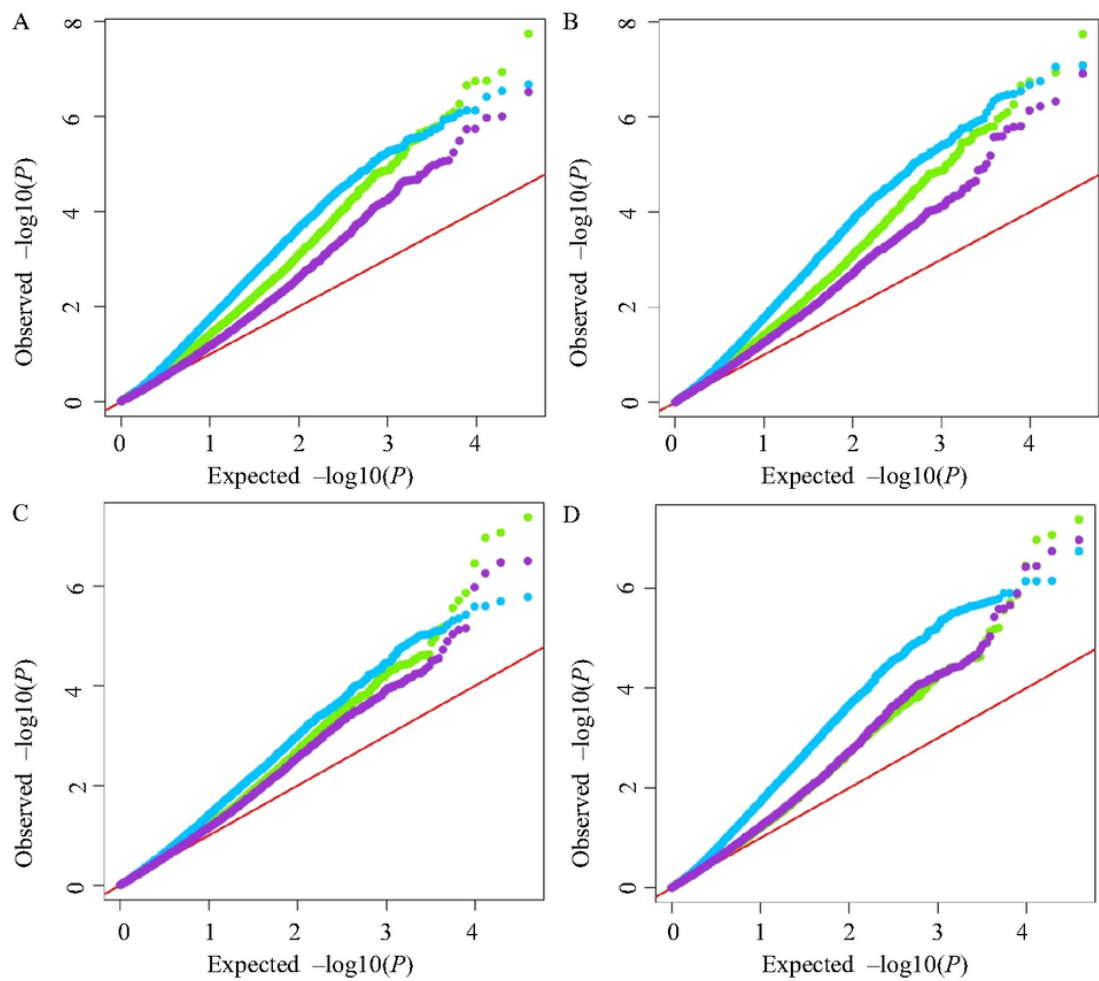


Figure 6

Quantile-quantile (QQ) plots resulting from GWAS results using three methods for leaf orientation value across three years A: Year of 2017; B: Year of 2018; C: Year of 2019; D: BLUP for combined three years. Green spots stand for Q model; Blue spots stand for K model; Purple spots stand for Q+K model.

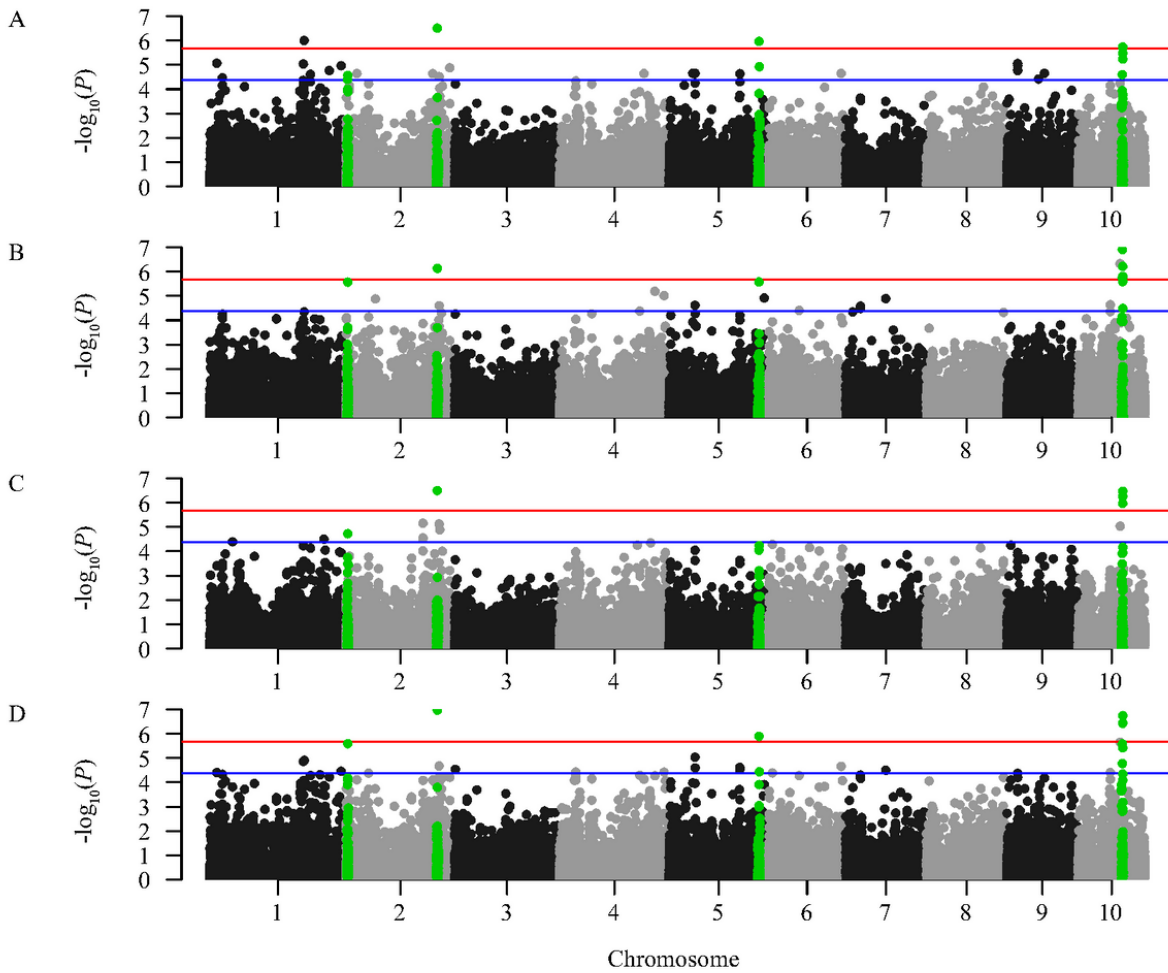


Figure 7
 The Manhattan plots of resulting from GWAS results using Q+K methods for leaf orientation value across three years A: Year of 2017; B: Year of 2018; C: Year of 2019; D:BLUP for combined three years.Green spots stand for the Manhattan plots of 50 SNPs in the upstream and downstream of lead SNP in bin 2.01, bin 2.07, bin 5.06 and bin 10.04 across three years. Blue lines were the threshold lines determined by GEC software